Jacek Górka, Andrzej Ozgowicz, Kamil Matusek

The Effect of Selected Spot Resistance Welding Parameters on Properties of Martensite-Structured AHSS

Abstract: The paper presents the effect of welding current and clamping force on the properties of spot resistance-welded joints made of 1.8 mm thick steel DOCOL 1200M. Because of the fact that martensite-structured steel DOCOL 1200M is hardened when exposed to deforming force, it is used to make energy absorbers or car header panels. Test joints, made using a robotic welding station, were subjected to macro and microscopic metallographic tests, hardness measurements and strength tests. The obtained test joints were subjected to strength verification performed in accordance with PN-EN ISO 14273:2016. The tests demonstrated that excessively high clamping force combined with relatively low welding current do not guarantee the obtainment of a joint characterised by required strength. However, by increasing welding current and reducing clamping force it is possible to increase the strength of welded joints. The use of appropriate spot resistance welding parameters enables the making of joints in steel DOCOL 1200M steel characterised by a satisfactory level of strength

Keywords: spot resistance welding, AHSS, steel DOCOL 1200M, martensite

DOI: *10.17729/ebis.2019.5/2*

Introduction

Presently, carmakers are strongly encouraged to reduce the kerb weight of manufactured vehicles. Efforts aimed at the reduction of weight are undertaken by design engineers aided by technologies enabling the selection of appropriate materials. As a result of material-related tests and the necessity of reducing the weight of vehicles, carmakers and other automotive sector companies increasingly often use aluminium alloys, composites and high strength steels. The primary requirements formulated by the automotive sector in relation to the above-named materials include the reduction of the weight of a component without compromising its mechanical properties, ability to absorb impact-accompanying energy, workability and good formability in terms of fusion and pressure welded joints. In addition, it is important that designed elements should be characterised by significant corrosion resistance and high fatigue strength. Steel DOCOL 1200M has been developed by the SSAB concern and is used by steelworks all over the world. Because of its high mechanical properties, the steel is rated among Advanced High Strength Steels

dr hab. inż. Jacek Górka (PhD (DSc) Habilitated Eng.), Professor at Silesian University of Technology;
mgr inż. Kamil Matusek (MSc Eng.) – Silesian University of Technology in Gliwice, Department of Welding;
mgr inż. Andrzej Ozgowicz, MSc Eng. – Styvo AS, STRYN, Norway

(AHSS). The steel is characterised by the presence of the dual-phase martensite-dominated structure and becomes hardened if exposed to deforming force. The foregoing leads to the shift of the yield point towards a relatively high level. As a result, the steel is used in the production of energy absorbers or car header panels. Because of the presence of the martensitic structure in the material, at the structure design stage, the structure should be appropriately optimised to avoid any form of the local bending effect. An additional advantage of the steel is its relatively low price resulting from a small amount of alloying agents [1–15].

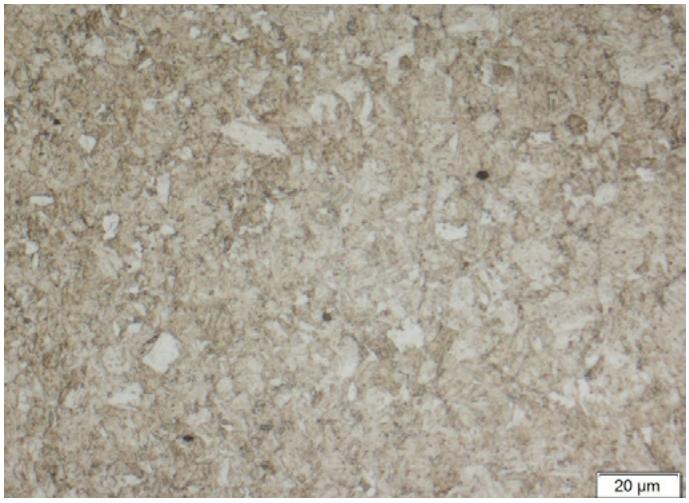

Fig. 1. Microstructure of steel DOCOL 1200M

Individual research

Research-related tests aimed to identify the effect of spot resistance welding parameters on the structure and properties of overlap joints made in 1.8 mm thick low-alloy high-strength martensitic steel DOCOL 1200M. The actual chemical composition and properties of steel DOCOL 1200M are presented in Table 1, whereas the structure of the steel is presented in Figure 1.

Welding process

Welded joints were made using a robotic spot resistance welding station at the ASKLA Maszyny i Technologie (Machinery and Technologies) company. The welding station was equipped with a KUKA KR180 robot with an ARO welding gun. A controller developed by the HARMS-WENDE company ensured the stability of parameters throughout the welding cycle. The tests involved the making of single overlap joints with two welds, characterised by the shape enabling the performance of shear tests and transverse tensile tests. The location of the welds was based on information contained in available standards and related reference publications. The parameters applied in the welding process are presented in Table 2.

Table 1. Chemical composition and mechanical properties of martensitic steel DOCOL 1200M

Contents of chemical elements, %											
C	Si	Mn	P	S	Al	Nb	V	Ni	Cr	N	Ce*
0.113	0.22	1.58	0.01	0.002	0.035	0.016	0.01	0.04	0.04	0.006	0.39
Mechanical properties											
Tensile strength R_m, MPa				Yield point R_e, MPa				Elongation A_{80}, %			
1260				1060				5			

* Ce – carbon equivalent

Table 2. Parameters applied during the welding of sheets made in steel DOCOL 1200M

Specimen designation	**Clamping force, kN**	**Welding current, kA**	**Welding current flow time, ms**	**Preheating current flow time, ms**	**Preheating current, kA**
A	2.5	8.5	600	0	0
B	1.5	10.0	400	0	0
C	1.5	10.0	300	200	2

Tests of welded joints

The welded joints were subjected to the following tests:

- macroscopic metallographic tests,
- microscopic metallographic tests,
- static shear test performed using an EDZ-20 testing machine, in accordance with PN-EN ISO 14273:2016,
- verification of strength in accordance with PN-EN ISO 14273:2016,
- Vickers hardness test-based hardness measurements performed in accordance with PN-EN ISO 14271:2011.

Analysis of test results

The macroscopic tests revealed that the applied welding cycle parameters were adjusted properly. The welded joint area did not reveal the presence of welding imperfections. The weld nugget was characterised by the proper shape and dimensions (see Figure 2).

The microscopic metallographic tests (Fig. 3–10) revealed that in the heat affected zone heated below temperature Ac1 there was an increase in the martensite tempering degree in relation to the structure of the base material.

Joint A

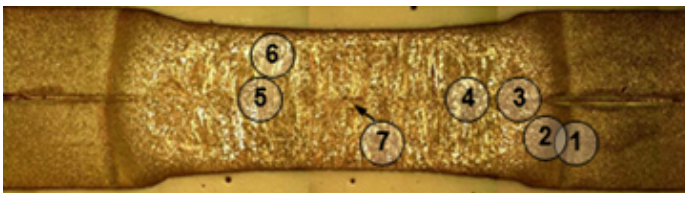

Joint B

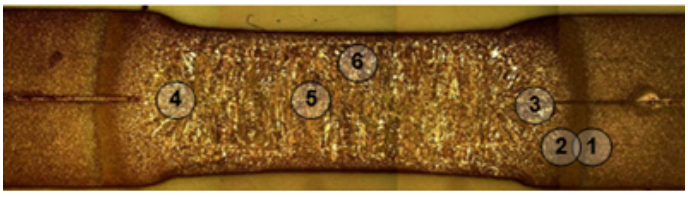

Joint C

Fig. 2. Macrostructure of the welds with points of microscopic photographs

In the area heated to temperature restricted within the range of Ac_1 to Ac_3, it was possible to observe the presence of martensitic or bainitic-martensitic islands against the background of high-tempered martensite. Along with a decreasing distance to the weld nugget and, consequently, an increase in temperature, the volume fraction of the islands increased until the entire recrystallization of the structure (exceeding of temperature Ac_3). The areas heated slightly above temperature Ac_3 were characterised by the presence of the fine acicular martensitic structure. Further HAZ areas revealed an increase in the thickness of martensite aciculae, which was connected with the growth of former austenite grains along with an increase in temperature. The weld was characterised by the coarse acicular bainitic-martensitic structure with a clearly visible primary columnar structure oriented towards heat discharge. The areas of the positive segregation of carbon and manganese, in the axis of the sheet, revealed the less intensively etched belt characterised by the martensitic-bainitic structure. The change in the structural morphology in the above-named area was related to the shift of the critical cooling curves towards higher time values along with an increase in the concentration of alloying elements dissolved in austenite.

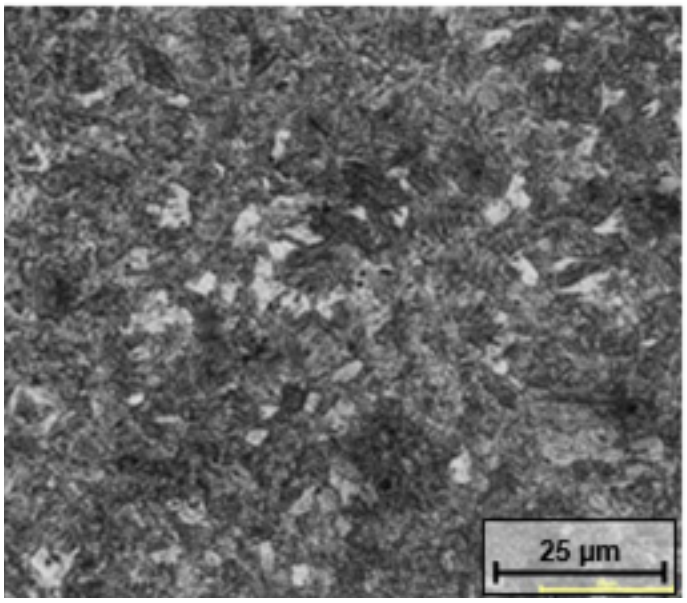

Fig. 3. Fine acicular structure of low-carbon martensite

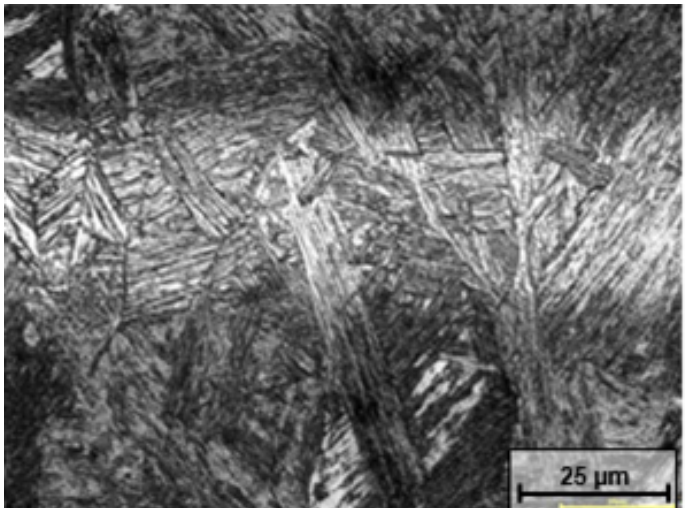

Fig. 4. Martensitic-bainitic structure in the area of the strip of the positive segregation of carbon and manganese in the sheet axis

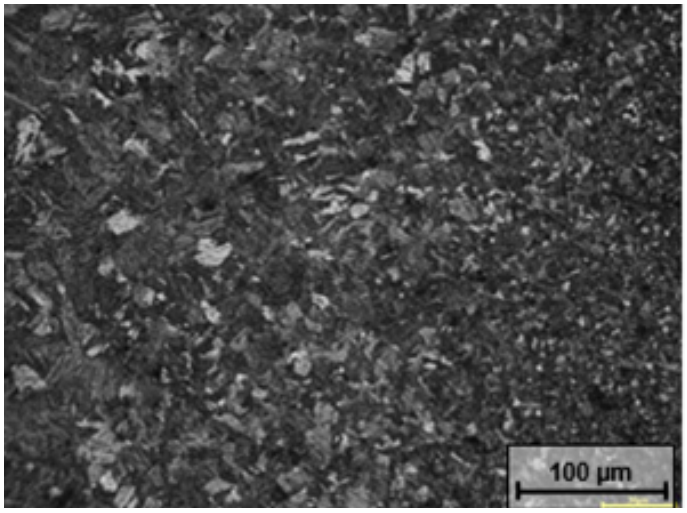

Fig. 6. HAZ; along with a decreasing distance to the weld nugget it is possible to observe an increase in the size of martensite aciculae; the foregoing is connected with an increase in the temperature of the micro-area and, consequently, the growth of former austenite grains (micro-area heating temperature Ac_3)

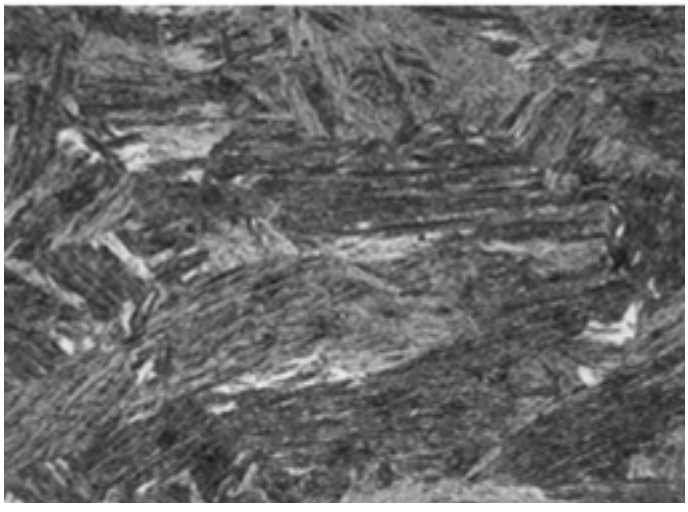

Fig. 8. Weld nugget; coarse-grained bainitic-martensitic structure; visible outline of the primary columnar structure oriented towards heat discharge

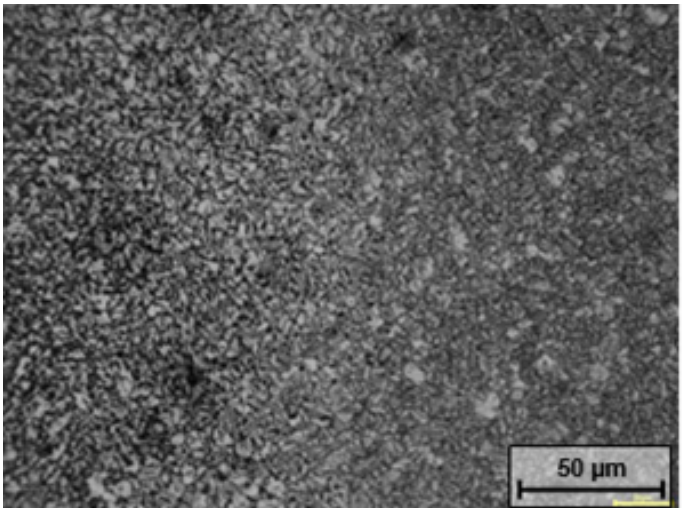

Fig. 5. HAZ; structure of tempered martensite (sorbite) – area heating temperature below Ac_1; along the grain boundaries it is possible to notice small, probably martensitic or martensitic-bainitic, islands – micro-area heating temperature between Ac_1–Ac_3

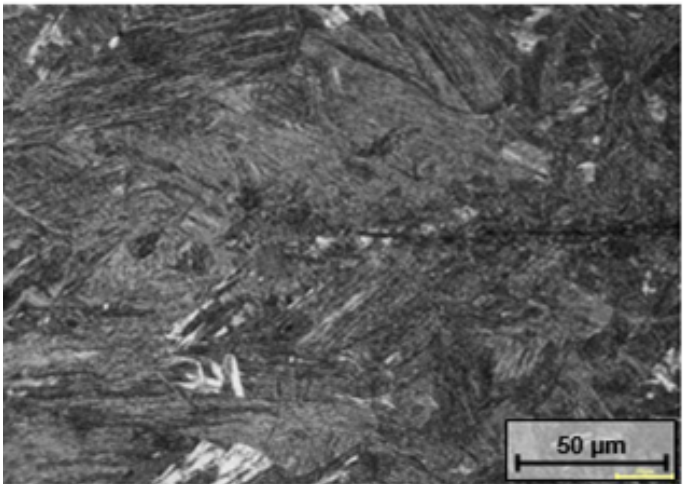

Fig. 7. Edge of the weld nugget: coarse-grained bainitic-martensitic structure; visible outline of the primary columnar structure oriented towards heat discharge

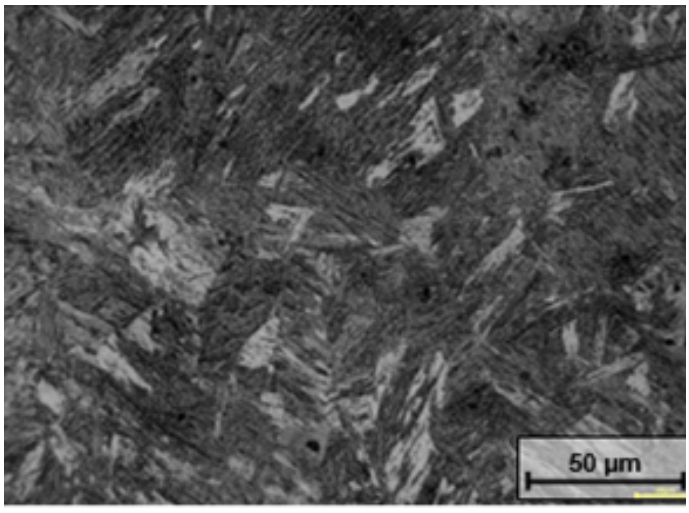

Fig. 9. Weld nugget; coarse-grained bainitic-martensitic structure; visible outline of the primary columnar structure oriented towards heat discharge

Verification of the strength of the joints

It is assumed that the welded joint should transmit shear force amounting to a minimum of 80% of the strength of the base material (in accordance with PN-EN ISO 14273:2016), (Table 3). The strength tests revealed that the base material should transmit a minimum shear force 86.4 kN.

When analysing the results of the strength tests it should be noted that specimen A, welded using a low current of 8.5 kA and a relatively high clamping force of 2.5 kN, did not meet the previously assumed boundary conditions. In turn, specimen C, previously subjected to preheating, transmitted the highest force, amounting to 90.9% of the base material. Specimen B, not subjected to preheating, transmitted shear force amounting to 81.6% (of the base material), which, given the characteristics of steel DOCOL 1200M, can be seen as a satisfactory result. In terms of strength, nearly all of the joints meet the strength-related assumptions (Fig. 11).

The hardness tests revealed the effect of changes in welding parameters on changes in hardness in individual areas of the joints (Figure 12). The highest difference between the mean value of the base material and the weld was observed in specimen A, i.e. the specimen welded using the lowest welding current (8.5 kA) and a relatively high clamping force of 2.5 kN. The hardness of the HAZ of the above-named specimen also proved to be the highest. The foregoing resulted from the fact that the specimen was subjected to the welding process characterised by the longest time of current flow of 600 ms. Therefore, it could be assumed that the growth of brittle martensite grains in the specimen was the greatest, which directly consistent with both strength and microstructural tests as the specimen was characterised by the lowest shear strength. Another specimen subjected to the hardness test was specimen B. It should be

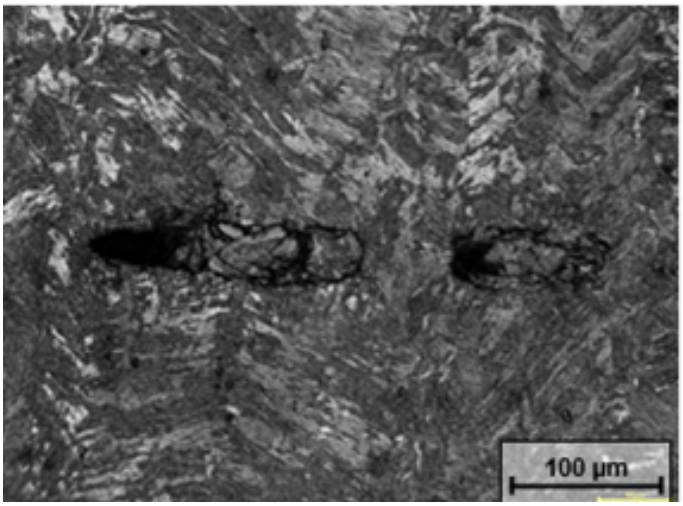

Fig. 10. Single local discontinuity in the welded joint

Table 3. Verification of boundary conditions for welded joints

Specimen no.	Shear force, kN	Base material strength
A	68.5 (6.85 tons)	86.4 (8.64 tons)
$F_{verification} = \frac{68.5x100}{86.4} = 79.8\%$		
The joint does not satisfy the strength-related criteria.		
B	70.5 (7.05 tons)	86.4 (8.64 tons)
$F_{verification} = \frac{70.5x100}{86.4} = 81.6\%$		
The joint satisfies the strength-related criteria.		
C	78.5 (7.85 ton)	86.4 (8.64 ton)
$F_{verification} = \frac{78.5x100}{86.4} = 90.86\%$		
The joint satisfies the strength-related criteria.		

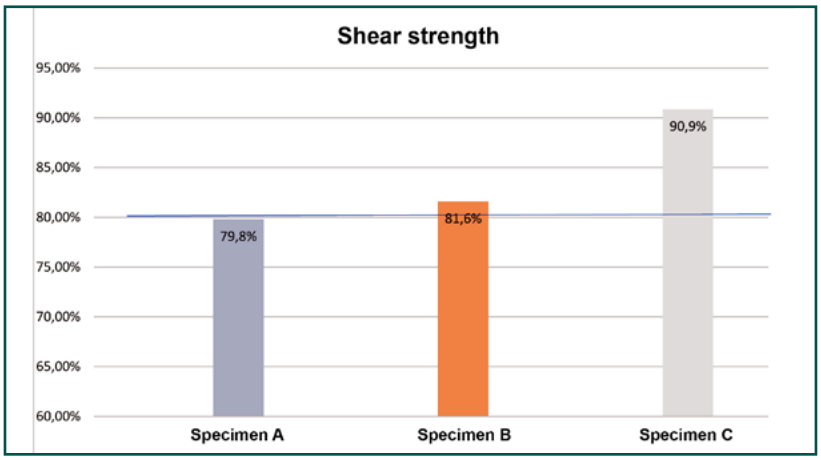

Fig. 11. Percentage shear strength of the welded joints in specimen A, B and C, where 100% represents the shear strength of the base material

noted that the mean hardness of the weld and that of the base material were nearly the same. Therefore, it could be assumed that an increase in welding current up to 10 kA combined with a simultaneous decrease in clamping force to 1.5 kN could improve the quality of the welded joint. It should also be noted that the reduction of the time of welding current flow to 400 ms significantly affected the hardness of the heat affected zone. As a result of the foregoing, based on the hardness measurement results and the results of the microstructural tests, it could be assumed that the smallest growth of the martensitic structure occurred in specimen B. The last specimen subjected to welding was specimen C. In general, the above-named element was made using parameters similar to those applied when making specimen B. The only difference was the preheating of the future joint area. A welding current of 10 kA and a clamping force of 1.5 kN made it possible to obtain the mean hardness of the weld similar to that of the base material. As regards specimen C, it was possible to observe the effect of preheating on the quality of the obtained welded joint. In spite of the application of parameters similar to those used when making specimen B, the hardness of the heat affected zone increased significantly. The foregoing was consistent with the strength test results, as the specimen transmitted the highest force related to the presence of largest weld nugget in the weld.

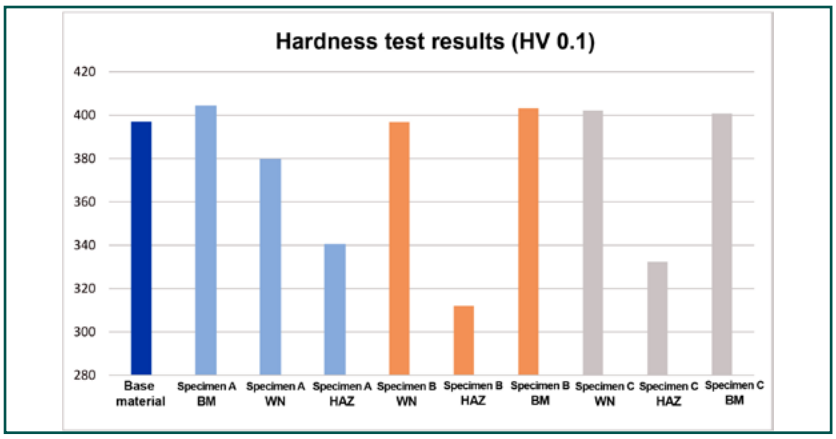

Fig. 12. Arithmetic mean of hardness measurements of specimen A, B and C; BM – base material, WN – weld nugget, HAZ – heat affected zone

Summary

The tests of the spot resistance welding of 1.8 mm thick steel DOCOL 1200M revealed the possibility of making welded joints satisfying related operational requirements. The appropriate adjustment of technological parameters makes it possible to obtain joints characterised by the proper shape of the weld nugget and mechanical properties satisfying the requirements of PN-EN ISO 14273:2016. The weld nugget area was characterised by coarse acicular bainitic-martensitic structure with clearly visible primary columnar structure oriented towards the discharge of heat. In the HAZ, the base material was tempered, leading to the formation of a softened zone, the hardness of which was by approximately 100 HV lower than that of the base material. The tests justified the formulation of the following conclusions:

- excessively high clamping force combined with relatively low welding current do not ensure the obtainment of welded joints characterised by required strength,
- increase in welding current combined with a decrease in clamping force increase the strength of welded joints,
- to reduce the probability of metal expulsion, it is necessary to identify an appropriate correlation between welding current and clamping force. It is assumed that an increase in welding current should be accompanied by a slight increase in clamping force,
- excessively long welding time leads to a significant increase in the size of the weld nugget, which could lead to the formation of welding imperfections in welded joints.

References

[1] Grajcar A., Różański M.: *Spawalność wysokowytrzymałych stali wielofazowych AHSS*. Welding Review, 2014, no. 3, pp. 22–27.

[2] Flaxa V., Shaw J.: *Material applications in ULSAB-AVC*. Steel Grips, 2003, vol. 1, no. 4, pp. 255–261.

[3] Krajewski S., Nowacki J.: *Mikrostruktura i właściwości stali o wysokiej wytrzymałości AHSS*. Welding Review, 2011, no. 7, pp. 45–50.
[4] Stano S.: *Spawanie laserowe blach o zróżnicowanej grubości przeznaczonych na półfabrykaty karoserii samochodowych typu tailored blanks*. Biuletyn Instytutu Spawalnictwa, 2005, no. 2, pp. 24–28.
[5] Chen B., Yu H.: *Hot ductility behaviour of V-N and V-Nb microalloyed steels*. International Journal of Minerals, Metallurgy and Materials, 2012, vol. 19, no. 6, pp. 525.
[6] Żuk M., Górka J., Czupryński A., Adamiak M.: *Properties and structure of the weld joints of quench and tempered 4330v steel*. Metalurgija, 2016, vol. 55, no. 4, pp. 613–616.
[7] Shipitsyn S., Babaskin Y., Kirchu I., Smolyakova L., Zolotar N.: *Microalloyed steel for railroad wheels*. Steel in Translation, 2008, vol. 38, no. 9, pp. 782–785.
[8] Godwin K., Yong O.: *Microstructure and fatigue performance of butt-welded joints in advanced high-strength steels.* Materials Science & Engineering A, 2014, vol. 597, pp. 342–348.
[9] Siewer A., Krastel K.: *Fiber Laser Seam Stepper Replacing Resistance Spot-Welding. A cost-effective laser based tool to conventional welding technology.* Laser Technik Journal, 2014, no. 4, pp. 52–55.
[10] Górka J., Ozgowicz A.: *Próby spawania laserowego niskostopowej wysokowytrzymałej stali o strukturze martenzytycznej.* Welding Review , 2016, vol. 88, no. 5, pp. 24–27.
[11] Senkara J.: *Współczesne stale karoseryjne dla przemysłu motoryzacyjnego i wytyczne technologiczne ich zgrzewania*. Welding Review, 2019, vol. 81, no. 11, pp. 3–7.
[12] Kaczmarek W., Panasiuk J.: *Zrobotyzowane procesy zgrzewania.* Control Engineering, 2015, no. 5, pp. 50–66.
[13] Zhang X.Y., Zhang Y.S., Chen G.L.: *Research on Weldability for Dual-Phase Steels Using Servo Gun Spot Welding System.* Key Engineering Materials, 2007, vol. 353–358, pp. 1597–1600.
[14] Kowieski S., Mikno Z., Pietras A.: *Zgrzewanie nowoczesnych stali o wysokiej wytrzymałości.* Welding Review, 2012, vol. 56, no. 3, pp. 46–51.
[15] Górka J., Ozgowicz A.: *Struktura i własności zgrzein punktowych stali* DOCOL *1200M.* Spajanie, 2018, vol. 1, no. 39, pp. 26–30.